PREVENTION OF GAS LEAKAGE THROUGH C/C COMPOSITE.

Hiroya Nagai *, Hiroshi Hatta **, Ken Goto **,Yasuo Kogo ***
*** Graduate Student Tokyo University of Science, ** ISAS/JAXA,**
***** Tokyo University of Science**

Keywords: *carbon-carbon composites, gas leakage, defect*

Abstract

Gas leakage through C/Cs was examined for the application of C/Cs to a combustion chamber of an ATR engine. Because C/Cs have many cracks and pores, gas easily leaks through the deffects. To predict and prevent this gas flow through the C/Cs, the leakage rates were measured as a function of pressure, and gas flow paths were identified by microscopic observations of C/Cs. On the basis of these results, gas flow models through C/Cs were proposed for unidirectionally (1D), 2-dimensionally (2D), and 3-dimensionally (3D) reinforced C/Cs. For the 1D- and 3D-C/C, the viscous flow models were found to be effective, and the labyrinth seal model was useful for 2D-Bare. Then, various methods for the prevention of the gas leakage through C/Cs were investigated. To this end, the combination of Si infiltration, sol-gel treatment, and glass coating over the surface was shown to significantly reduce leak rate, and to be sufficient for combustion chamber application.

1 Introduction

Carbon fiber reinforced carbon matrix composites (C/Cs) consist of carbon matrix reinforced with carbon fiber. C/Cs maintain excellent strength, toughness, and heat shock resistance at temperatures exceeding 2000K. Due to these advantages, C/Cs are expected to be applied to structures exposed to high-temperature environments especially in aerospace field [1]. For example, at the Institute of Space and Astronautical Science, Japan, an study to apply C/Cs to the combustor for a future space plane engine, an air-turbo-ram-jet (ATR) engine, is underway [2]~[4]. This engine will propel a space plane by burning a mixture of hydrogen fuel and oxygen in the atmosphere. If C/Cs are applicable to the combustor, the ATR engine can possesses much lower weight and higher temperature capability. However, C/Cs are inherently porous materials. In applications of C/Cs to such an airtight structure as combustion chamber, it is afraid that fuel (H_2 gas) and/or combustion gas may leak through these defects in C/Cs [4], which results in loss of operation efficiency of an engine system or explosion of total system. Thus, it is one of key issue to minimize the amount of the gas leakage through a C/C for example until the requirement (pressure: 2MPa, leak rate: 9.2 x 10^{-4}[kg/s/m^2]) for the combustor of the ATR.

In the present study, in order to identify the gas leak routes, cross-sections of C/Cs were observed in detail. On the basis of this result, gas flow models through C/Cs were proposed and calculated gas flow rates using the gas leak model were compared with experimental results as functions of pressure. Then, measures for the prevention of gas leakage through 3D-C/C were studied in order to apply C/Cs to the combustion chamber of the ATR engine.

2 Leak analysis

2.1 Leak paths

C/Cs examined in the present study included unidirectionally reinforced, cross-ply-laminated, and three-dimensionally reinforced composites. Hereafter, these C/Cs are referred to as 1D-Bare, 2D-Bare, and 3D-Bare, respectively. In order to diminish gas leak, Si was infiltrated in defects distributed in the C/Cs. In the Si infiltration treatment, an excess amount of Si plates was put the upper surface of a C/C, 30 x 30 x 15 mm, and heated at 1873 K (T_0), which was higher than the melting point of Si, 1687 K under reduced pressure environment less than 5×10^{-4} Torr. Then, Si was easily infiltrated into defects in C/Cs. In this treatment, the maximum temperature was maintained for 1 hour. Gas leak tests were carried out after the removal of excess Si and SiC converted

on the surfaces of the Si-infiltrated C/Cs by polishing using diamond past. Hereafter, these C/Cs are referred to as 1D-Si, 2D-Si, and 3D-Si.

2.2 Leak test

Experimental set-up for the determination of gas leak rate through C/Cs is schematically illustrated in **Fig. 1**. The C/C specimen for the leak test was a thick disk of 24 mm in diameter and 10 mm in thickness. The specimen was carefully bonded to a sample holder with epoxy adhesive to avoid gas leak through the gap between the sample and its holder. In order to make adhesive layer crack free, the gap was controlled less than 0.1~2 mm. Then, a specimen-bonded holder was set in a pressure proof chamber sealed by O-rings, and high pressure was applied from one side. The gas-flow rates through the sample were determined using a gas flow meter. To estimate gas leakage through the epoxy adhesive layer, preliminary leak tests were performed using a metal plate specimen. It was thus assured that the gas leak through the bonding layer could be ignored compared with that through the C/C specimens. Although the operation gas of the heat exchanger for the ATREX is hydrogen, nitrogen gas was used for safety. The applied pressure was up to 5 MPa, which was determined from requirement for the actual heat exchanger in the ATREX (up to 2MPa). All the gas leak tests were conducted at room temperature.

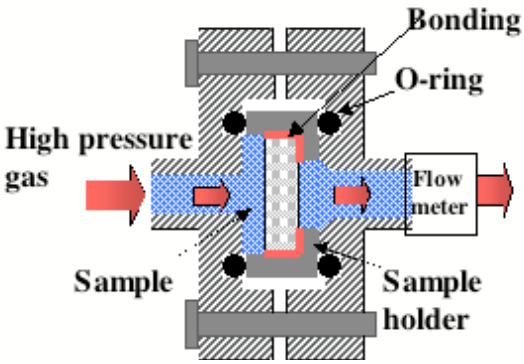

Fig.1 Schematic of leak-rates measurements at Room temperature.

2.3 Leak analysis

2.3.1 1D-C/C

The gas-leak paths in the fiber-axis direction of the 1D-Bare and 1D-Si were regarded as the elongated voids. Thus, the gas flow through a circular pipe was assumed to be a suitable leak model for the 1D-Bare and 1D-Si. Flow within a pipe is known as Poiseuille flow. The pressure difference between the inlet and exit of the leak flow, is large, and the operation fluid is a gas. Thus, the compressibility of the gas was taken into consideration. The force equilibrium for compressive fluid through a circular pipe, radius R, is given by:

$$U = -\frac{R^2}{8\mu}\frac{dp}{dx} \qquad (1)$$

where U, R, p, m, and x stand for the average velocity, the diameter of the circular pipe model gas pressure, viscosity, and axial coordinate, respectively. Equation (1) can be integrated using the well-known condition of Pv = constant to result in eq. (2) and (3).

$$\overline{U} = \frac{R^2}{16\mu Lp}\left(p_i^2 - p_0^2\right) \qquad (2)$$

$$p = \sqrt{\frac{1}{L}\left(p_i^2 - p_0^2\right)x + p_0^2} \qquad (3)$$

where, the specific volume is denoted by v, the thickness of C/C by L, and the maximum and minimum pressures by p_i and p_0 [Pa], respectively.

2.3.2 2D-C/C

The labyrinth seal is composed of many abrupt conversing and diverging sections in the flow path. The gas passing through this seal repeats adiabatic compression and expansion to yield flow resistance, and so gas leak is minimized. The transverse cracks in the 2D-Bare, -Si can be regarded as expanding sections, and the joining sections of two transverse cracks as compressing sections, the leak path in the 2D-C/C is similar to that of a labyrinth seal [5] as shown in Fig. 2. Assuming ideal adiabatic expansion and compression of gas and n steps of a labyrinth, a leak rate from the seal is given by eq. (4).

$$G = \alpha_i F_i P_{i-1}\sqrt{\frac{K_{i-1}}{K_{i-1}-1}\frac{1}{RT_{i-1}}\left\{\left(\frac{P_i}{P_{i-1}}\right)^{\frac{2}{K_{i-1}}} - \left(\frac{P_i}{P_{i-1}}\right)^{\frac{K_{i-1}+1}{K_{i-1}}}\right\}} \qquad (4)$$

$$\left(\frac{2}{\kappa_{i-1}+1}\right)^{\frac{\kappa_{n-1}}{\kappa_{n-1}-1}} \qquad (5)$$

where G: mass flow rate [kg/s], α : flow coefficient (0.6~1.0), F: area of contracted sections [m^2], R: gas constant [J/kg/K], T: temperature [K], P: pressure [Pa], κ : Specific heat ratio, suffix i: labyrinth steps (1~n, 0: just upstream of labyrinth). Because the mass flow rate is common in each stage, explicit expression of eq.(5) turns into simultaneous

equations of n rank.). When P_i/P_{i-1} becomes lower than the critical pressure ratio eq.(6), P_i/P_{i-1}. is set to the critical pressure ratio given by eq.(5). In these equations, α, F, κ, R, T, P_0, and P_n are known quantities, and G and pressures P_1~P_{n-1} are n unknowns. Thus, eq. (5) can in principle be solved. The numerical values used for the above calculations were as follows. F is the contact area of transverse cracks multiplied by the number of the contacts per unit area of sample. The contact area and its density were predetermined by microscope observations of the 2D-C/C. The flow coefficient α is affected by the shape near the edges of the compressive sections and their surface coarseness. The opening width of transverse cracks tends to narrow when approaching interlamina, contact areas. Such shapes facilitate converging flow and make α small. In addition, coarse surfaces of transverse cracks also make α smaller. Usually α takes a value from 0.6 to 1.0, and the minimum value of α, 0.6, was adopted in the present calculations. Strictly speaking, the specific heat ratio κ is a function of pressure and temperature. However, such dependencies of nitrogen and helium are very weak. Thus, the specific heat ratios at room temperature under atmospheric pressure, nitrogen; 1.40 and helium; 1.66 were used.

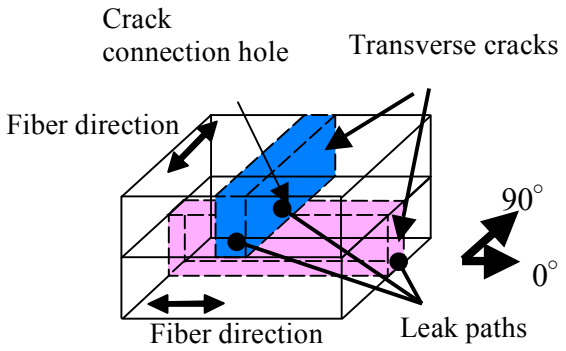

Fig.2 Schematic illustration of gas-leak paths in 2D-C/C.

2.3.3 3D-C/C

The major gas-leak paths in the 3D-Bare and 3D-Si ware found to be transverse cracks (TCs) in fiber bundles and debonding along fiber-bundle interfaces orienting parallel to the leak direction (IDs). These cracks ran straightly through the whole thickness. Thus compressive flow between parallel plates was adopted for the leak through 3D-C/Cs. The Poiseuille flow can be solved by a procedure similar to that used for the circular pipe flow, and esq. (6) - (8) were obtained.

$$U = -\frac{H^2}{12\mu}\frac{dp}{dx} \tag{6}$$

$$\overline{U} = \frac{H^2}{24\mu Lp}\left(p_i^2 - p_0^2\right) \tag{7}$$

$$p = \sqrt{\frac{1}{L}\left(p_i^2 - p_0^2\right)x + p_0^2} \tag{8}$$

Here, L: thickness of C/C [m], x: position in the flow direction [m], H: crack opening [m]. In the calculations using these equations, the crack-opening area was approximated by long rectangles, and Hs and the crack lengths (Ls) were independently determined for the TCs and IDs on cross-sections of the 3D-C/C.

3 Results and discussion

3.1 Cross-section of C/Cs

Typical cross-sections of the examined C/Cs are shown in Fig.3. In the 1D-B (Fig.3 (a)), fiber-scale voids extended along fibers. In the 2D-Bare, large transverse cracks ran parallel to fibers. These transverse cracks extended across the whole thickness of each lamina and ran the whole length of the original plate in the in-plane direction. The transverse cracks were generated during the fabrication stage for the material due to anisotropic shrinkage of the matrix in the carbonization process and also due to differences in thermal expansion between a 0° and 90° layers during cooling stage from the HTT.

In the 3D-Bare, the cross-section of fiber bundles had different pattern depending on the cutting direction. As Fig.3(c) shows, the cross-section of fiber bundles oriented in the x direction deformed into a long ellipsoidal shape, where big cracks orienting parallel to fiber ware observed. The similar deformation was observed in y-bundles. In contrast, the cross-sectional shape of the z-axis fiber bundle was a nearly square, where debonding along fiber-bundle interfaces orienting parallel to fiber ware observed. These cracks ware assumed to be the major gas-leak path. In the 1D-, 2D-, 3D-Si, major cracks were almost filled with SiC formed by the reaction of infiltrated Si with carbon in the C/C as shown Fig.3 (d), (e), (f). However, smaller numbers of small cracks without filling SiC are observed. These narrow cracks were very likely produced during the Si infiltration process. This manifests that gas leak paths are not completely sealed by the Si infiltration.

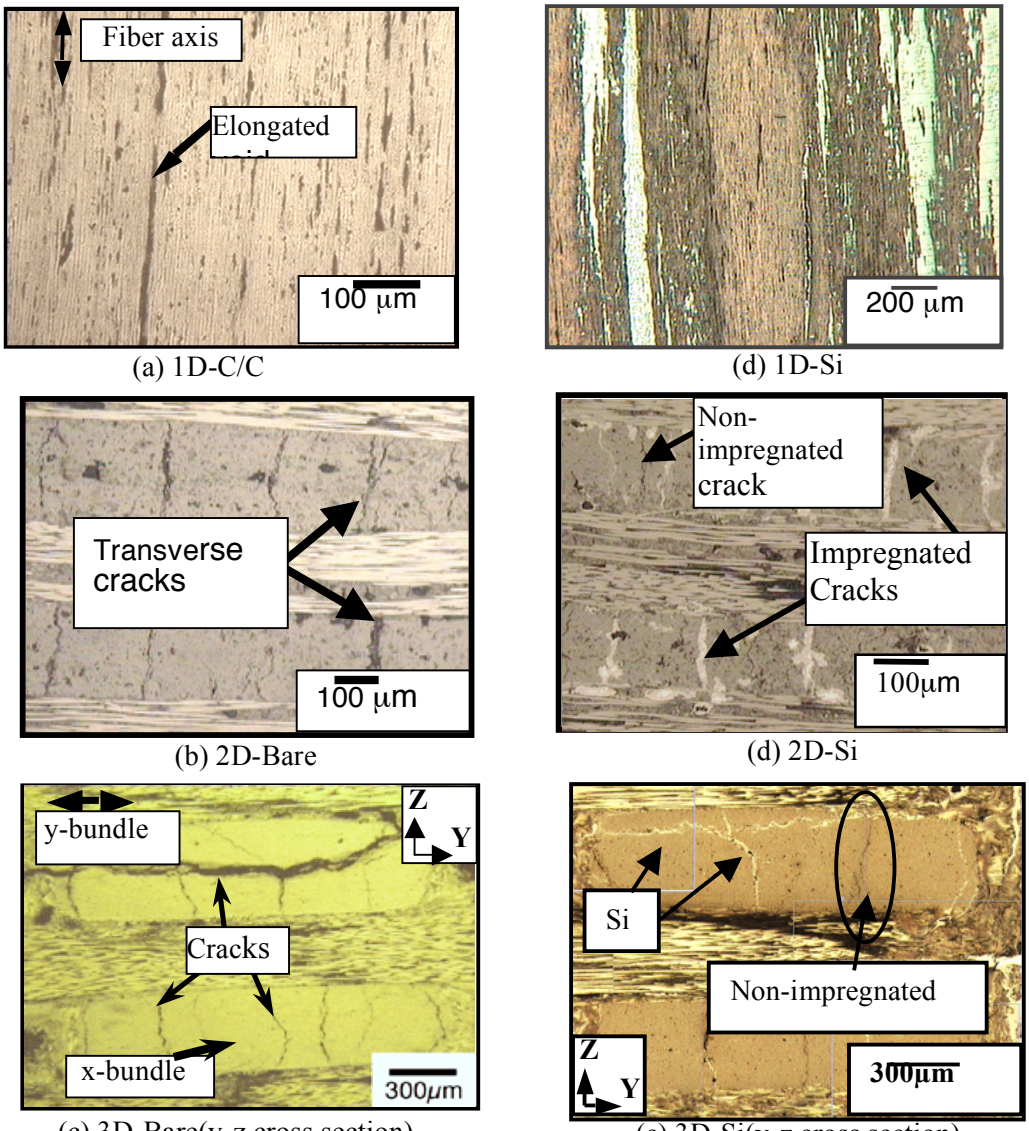

Fig.3 Cross-sections of the (a)1D-, (b)2D-, (c) 3D-C/C (y-z cross section),and (d)1D-,(e)2D-,(f)3D-Si (y-z cross section).

3.2 Comparison between prediction and leak rate result

3.2.1 1D-C/C

In Fig. 4, observed and predicted gas leak rates through the 1D-Bare and 1D-Si C/Cs are compared. In the calculations, we used the average values of diameter for the 1D-Bare and 1D-Si of 8.1 μm and 2 μm, and void rate of 9.5% and 6.9%, respectively. Actual defects have an irregular periphery. The longest and shortest dimensions of void cross-sections were measured, and the diameter of the model pipes was determined using average. The void rate was determined by image analysis. As this

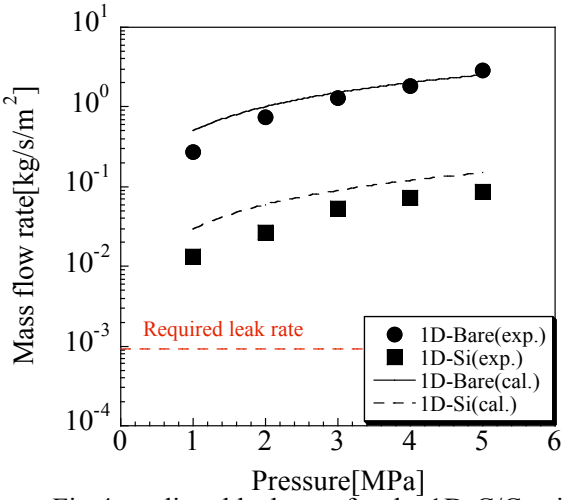

Fig.4 predicted leak rate for the 1D-C/C using the circular pipe model and experimentally determined results.

figure shows, the calculation results reasonably agree with the experimental values. Thus, the viscous flow model in a circular pipe is concluded to be effective for the predictions of gas-leak rates in the 1D-C/C in the fiber-axis direction.

3.2.2 2D-C/C

The predicted gas-leak rates of the 2D-Bare and 2D-Si are compared with the experimental values in Fig. 5. In this calculation, the average values of opening width of the transverse cracks for the 2D-Bare and 2D-Si were 9.5 μm and 2.1 μm, and the crack spacing were 320 μm and 350 μm, respectively. As this figure shows, the calculation results reasonably agree with the experimental values about 2D-Bare. In contrast, about 2D-Si, the calculation results don't agree with the experimental values.

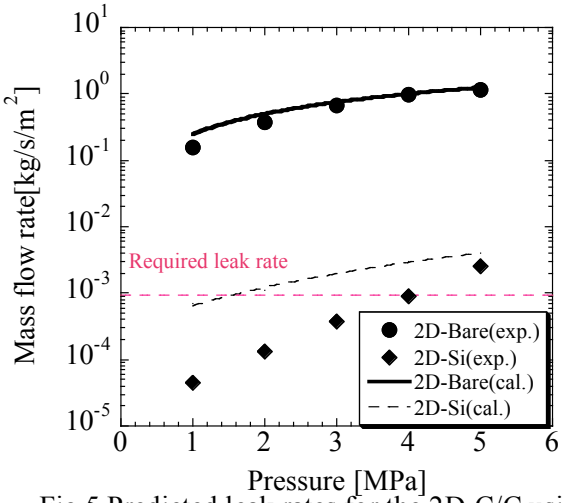

Fig.5 Predicted leak rates for the 2D-C/C using the labyrinth seal model and experimentally determined results.

3.2.3 3D-C/C

The results, which compare the predicted mass leak rates and the actually observed values at the exit, are shown in Fig. 6. The average crack opening (h), crack length (L), and volume fraction of cracks (V_c) are shown in Table 1. As this figure shows, the calculation results reasonably agree with the experimental values.

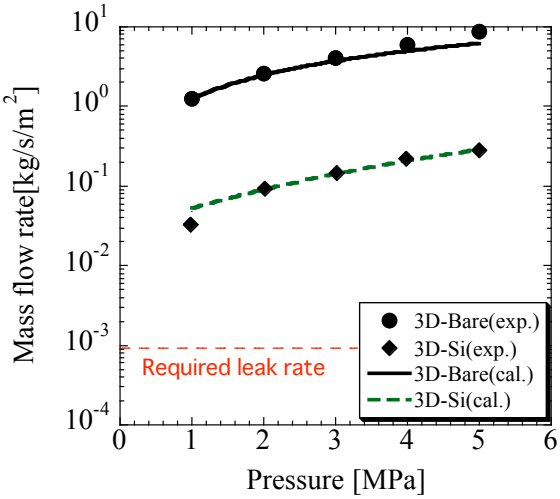

Fig.6 Comparison between predicted leak rates through the 3D-C/C using the parallel plates model and experimentally determined values.

3.3 The Effects of sol-gel treatment on leak rate

As Fig.4, 5, and 6 show, 3D-C/C was found to exhibit much higher gas leak rate than the other C/Cs. Despite the Si infiltration yielded large reduction in gas leak rates, the leak level of the 3D-C/C still does not satisfy the required leak rate for the combustion chamber.

Interlaminar strength of C/C is very low, so that 3D-C/C has been generally used in practical applications of C/Cs [6][7], especially the cases required high performance. Therefore, It is absolutely important to minimize gas leak rate through 3D-C/Cs.

The reason for the restrictive effect of the Si infiltration on gas leakage is presence of the un-infiltrated cracks. Such cracks remains after the Si infiltration, because of thermal expansion mismatch between the regions of fibers lying different

Table.1 Average width h and length L, and volume fraction of cracks V_c in 3D-C/Cs.

Material	*xy*-cracks			*zx*-cracks		
	Width, W [μm]	Length, L [μm]	Content, V_c [Vol. %]	Width, W [μm]	Length, L [μm]	Content, V_c [Vol. %]
3D-Bare	16.9	1075	1.4	9.3	345	0.45
3D-Si	9.9	860	0.18	4.8	291	0.076

directions. The thermal expansion mismatch relieves with increasing temperature until the heat treatment temperature, the width of the cracks in C/C decreases with rising temperature. Thus, even if Si was completely infiltrated at elevated temperature, cracks reopened when temperature was down to room temperature. For this reason, we believe that the filling material into remainig crack at the low temperature is effective to fill completely the remaining defects.

The sol-gel method was examined for further filling the remaining voided spaces in Si-infiltrated C/Cs aiming at further minimizing the amount of the gas leakage. In Sol-gel treatment, the SiO_2 glass was formed in the defects of a 3D-C/C-Si by dipping the C/C in a gel solution. In order to facilitate the filling in defects, dipping was repeated ten times under reduced pressure environment. For a part of specimens, sol-gel coating was finally applied on the surface in order to further minimize the gas leak rate.

The gas leak rates of sol-gel treated C/Cs are shown in Fig.7 as a function of gas pressure, where Bare is untreated C/C, Si is Si-infiltrated C/C, SiO_2 is sol-gel-treated C/C, and SiO_2+film is the C/C applied the combination processes of Si infiltration, sol-gel treatment, and glass coating over the surface. As this figure shows, additional SiO_2 infiltration by sol-gel treatment yielded reduction in the gas leak rate more than one order of magnitude comparing with only Si treatment. However, this level still does not satisfy the required leak rate for the combustion chamber. The satisfactory leak levels was obtained after further glass coating applied over the surface.

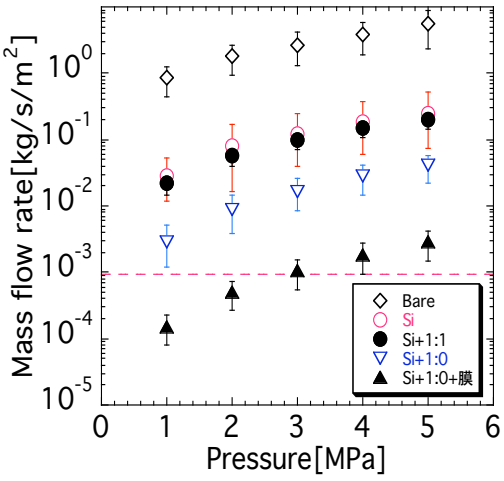

Fig.7 Gas leak result of bare C/C and Si, sol-gel treated C/Cs.

4 Conclusions

In order to understand gas leakage through C/Cs, the gas leak routes were at first identified. On the basis of this result, gas flow models through C/Cs were proposed and calculated gas flow rate was compared with experimental results as a function of pressure. Then, various methods for the prevention of the gas leakage through 3D-C/C were investigated. The major conclusions obtained in the present study are as follows.

- The major gas leak paths in uniderectionally reinforced C/C are elongated voids between fibers, and those in three-dimensionally reinforced C/Cs are transverse cracks and interfacial debonding between fiber bundles. For both C/Cs, the viscous flow models are shown to be effective for leak-rate predictions.
- The major gas-leak paths in cross-ply-laminated (2D-) C/C are transverse cracks, and the leak rates can be predicted by the labyrinth seal model. However, for Si infiltrated 2D-C/C, the calculation results did not agree with the experimental values.
- The leak levels of the specimens formed by combination processes of Si infiltration, sol gel treatment, and glass coating over the surface, satisfied the required leak rate for a combustion chamber under pressure lower than 2MPa.

References

[1] Inagaki M. "*New Carbon Materials (in Japanese)*". Gihodo Pub. Japan, pp.185~194 1994.

[2] Sato T, Tanatsugu N, Hatta H, Goto K, Kobayashi H, Omi J, Tomike J. "Development Study of the ATREX Engine for TSTO Spaceplane". *10th International Space Planes and Hypersonic Systems and Technology Conference*; 2001, AIAA-2001-1839, 2001

[3] Hatta H, Goto K, Kogo Y, Ichikawa M. "Heat exchangers for Air-Turbo-Ram-Jet Engine". In: Krenkel W, Naslain R, Schneider H, editors. Proceedings. *High Temperature Ceramic Matrix Composites*, Vol.4, Munich; 2001; pp.797-801

[4] Nishiyama Y, Hatta H, Bando T, Sugibayashi T. "The Gas Leakage Analysis in C/V Composites." *JIAA J.* 2002; 50(587); 483-488

[5] Komotori K. "Air flow through labyrinth seal (in Japanese)". *Trans. JSME* 21-105(1955). 377-382.

[6] Hatta H, Goto K, Kogo Y, Ichikawa M. "Heat exchangers for Air-Turbo-Ram-Jet Engine". In: Krenkel W, Naslain R, Schneider H, editors. Proceedings. *High Temperature Ceramic Matrix Composites*, Vol.4, Munich; 2001; pp.797-801

[7] Y. Nishiyama, H. Hatta, T. Bando, T. Sugibayashi. “The Gas Leakage Analysis in C/C Composites”. *J. Japan Soc. Aeronautical and Space Science (in Japanese)* 2002; vol. 50(587), pp. 483-488

[8] Sakka S. “Chemistry of Sol-gel method”. Agnesyoufusya: pp.5～12 1990

[9] Tomita Y. “Introduction to hydrodynamics”. Youkendou; 1971 pp.30